AEM
Journals.ASM.org

Analysis of Structure and Composition of Bacterial Core Communities in Mature Drinking Water Biofilms and Bulk Water of a Citywide Network in Germany

Karsten Henne, Leila Kahlisch, Ingrid Brettar, and Manfred G. Höfle

Department of Vaccinology and Applied Microbiology, Helmholtz Centre for Infection Research (HZI), Braunschweig, Germany

The bacterial core communities of bulk water and corresponding biofilms of a more than 20-year-old drinking water network were compared using 16S rRNA single-strand confirmation polymorphism (SSCP) fingerprints based on extracted DNA and RNA. The structure and composition of the bacterial core community in the bulk water was highly similar (>70%) across the city of Braunschweig, Germany, whereas all biofilm samples contained a unique community with no overlapping phylotypes from bulk water. Biofilm samples consisted mainly of *Alphaproteobacteria* (26% of all phylotypes), *Gammaproteobacteria* (11%), candidate division TM6 (11%), *Chlamydiales* (9%), and *Betaproteobacteria* (9%). The bulk water community consisted primarily of *Bacteroidetes* (25%), *Betaproteobacteria* (20%), *Actinobacteria* (16%), and *Alphaproteobacteria* (11%). All biofilm communities showed higher relative abundances of single phylotypes and a reduced richness compared to bulk water. Only biofilm communities sampled at nearby sampling points showed similar communities irrespective of support materials. In all of our bulk water studies, the community composition determined from 16S rRNA was completely different from the 16S rRNA gene-based community composition, whereas in biofilms both molecular fractions resulted in community compositions that were similar to each other. We hypothesize that a higher fraction of active bacterial phylotypes and a better protection from oxidative stress in drinking water biofilms are responsible for this higher similarity.

Biofilms are present in every drinking water distribution system (DWDS), and they are attached to the surface of tubing material of the distribution network (3). Biofilms can be of great relevance for public health, because many potentially pathogenic bacteria are not located in the bulk water but are in the biofilm of the pipes, where they are more protected against adverse environmental conditions, such as disinfection measures (7, 38, 41, 44). Especially in the case of pressure loss events, the shear stress can disrupt pieces of biofilm, not only giving an unpleasant color and flavor to the bulk water but also creating a potential health risk (10, 37).

Many studies have focused on the examination of artificial drinking water biofilms in model systems (22, 26, 29). Assuming that only minor changes occur after a rather stable biofilm has developed, most biofilm studies concentrated on short periods with biofilms growing for only a few months. However, Martiny et al. (29) showed that a stable community of a drinking water biofilm needed years to be established. For young biofilms it is reported that different tubing material of model DWDS, such as copper, PVC, or stainless steel, may affect the number of cells, the morphology, and the bacterial composition (10, 24, 38, 39). Various pathogens, such as *Legionella pneumophila*, *Mycobacterium* spp., and *Helicobacter* spp., were observed to be primarily associated with or grow in biofilms (4, 10, 12, 32). Therefore, drinking water biofilms are considered an important reservoir for pathogens and a source of bulk water contamination (25).

Cultivation-independent methods have been developed using 16S rRNA gene-based approaches to identify bacterial species and assess their abundances within drinking water communities (3, 6). For example, molecular fingerprints using single-strand confirmation polymorphism (SSCP) electrophoresis allow a rapid and economic overview of the bacterial core community, i.e., the bacterial species with relatively high abundances (e.g., a detection limit of 0.1% for single members of the bacterial community is currently assumed for fingerprints [14]). Focusing on the abundant bacterial species seems reasonable, because the main members are presumed to be the key drivers of processes in water and biofilm (5). Molecular fingerprints allow us to describe structural features such as the relative abundance of a single species, the richness, and the evenness of a community (6, 9). DNA-based techniques targeting 16S rRNA genes are generally used to assess the presence and the relative abundance of single phylotypes (PTs). On the other hand, the 16S rRNA concentration is dependent on the ribosome content of the bacterial cell, which rises with increasing growth rate or activity, and is currently understood to be an indicator of bacterial activity (35). Therefore, the use of RNA-based fingerprints could help to screen for active phylotypes and/or to detect low-abundance but active phylotypes that are not detected by DNA-based techniques (11, 21, 23, 27).

The present study aimed at understanding the community structure and composition of the bacteria in drinking water biofilms compared to those in bulk water. To this end, mature biofilm was sampled from different pipe materials at different locations in a small-scale network in continuous use for 20 years to assess spatial heterogeneity (11, 17, 21). By comparing DNA- and RNA-based fingerprints, we wanted to test the hypothesis that biofilms show the same complete differences between these two types of

Received 29 July 2011 **Accepted** 22 February 2012
Published ahead of print 2 March 2012
Address correspondence to Manfred G. Höfle, mho@gbf.de.
Supplemental material for this article may be found at http://aem.asm.org/.

doi:10.1128/AEM.06373-11

fingerprints as the bulk water (11). If this was not the case, it would mean that the biofilm communities have different structure-function relationships than the bulk water communities.

MATERIALS AND METHODS

Study sites and sampling. Bulk water was sampled on 23 and 24 June 2009 from several taps distributed around the campus of the Helmholtz Centre for Infection Research (HZI), Braunschweig-Stöckheim, Germany (T-HZI-1 to T-HZI-5), and from 2 households of the inner city of Braunschweig (T-BS-1 and T-BS-2) (see Fig. S1 and Table S1 in the supplemental material). Biofilm samples (B-HZI-2 and B-BS-1) were taken in parallel to the bulk water sampling. Additional biofilm samples (B-HZI-1 and B-HZI-3 to B-HZI-6) were obtained on 7 and 14 May 2009, when the L building at the HZI campus was dismantled (see Fig. S1 and Table S2 in the supplemental material). All bulk water or biofilm samples were from the following three different water networks connected to the HZI campus. (i) The municipal water network, which is a network supplying the whole city of Braunschweig, including the HZI campus. (ii) The main network at the HZI campus, which is a circular network supplying most of the buildings on the HZI campus. This network is connected to municipal water, including a pressure reducer and filter. (iii) Looped fire water mains, a network that supports fire hydrants and a few buildings on the HZI campus. It is connected directly to the municipal water. The drinking water originated from two surface water reservoirs (oligotrophic and dystrophic water) situated in a mountain range 40 km south of Braunschweig. The processing of the drinking water by the local supplier Harzwasserwerke GmbH included flocculation/coagulation, sand filtration, and chlorination (0.2 to 0.7 mg liter^{-1}). More details on the respective drinking water supply systems are given elsewhere (11).

Drinking water microorganisms were sampled by filtration according to Eichler et al. (11). In brief, 5 liters of drinking water was filtered through a filter sandwich consisting of a 0.2-μm-pore-size polycarbonate filter (90-mm diameter; Nuclepore; Whatman, Maidstone, United Kingdom) with a precombusted glass fiber filter on top (90-mm diameter; GF/F; Whatman). Biomass harvested on filter sandwiches was stored at −70°C until further analysis. In parallel, heterotrophic plate counts (HPCs) and direct counts were performed, and relevant drinking water parameters, such as pH, conductivity, temperature, and chlorine concentration, were determined (see Table S1 in the supplemental material). Using sterile swabs (Heinz Herenz, Hamburg, Germany), drinking water biofilms were wiped off the wet surfaces of the tubing of different sampling locations and different materials. Swab heads with biofilm material were stored in 1.5-ml reaction tubes at −70°C until further analysis (see Table S2).

Heterotrophic plate counts and direct counts of drinking water bacteria. HPCs were done in triplicate using an aliquot of the drinking water and the spread plate technique on R2A agar (Oxoid) plates. Incubation was carried out at two different temperatures according to the German drinking water ordinance (36°C for 48 h and 20°C for 72 h).

For total bacterial cell counts, formaldehyde-fixed samples (2% final concentration) were stained with Sybr green I dye (1:10,000 final dilution; Molecular Probes, Invitrogen) for 15 min at room temperature in the dark. Five ml was filtered onto 0.2-μm-pore-size Anodisc filters (Whatman) and mounted with Citifluor on microscopic glass slides according to Weinbauer et al. (43). Slides were either analyzed directly with epifluorescence microscopy or stored frozen (−20°C) until examination. For epifluorescence microscopy, a microscope (Axioplan, Zeiss) with suitable fluorescence filters was used, and the slides were examined using 100-fold magnification. For each sample, 10 micrographs were taken and image sections of defined size (0.642 by 0.483 mm) were analyzed using Image J software with the plug-in collection from MacBiophotonics (http://www.macbiophotonics.ca/). Typically, 500 to 800 bacterial cells per image were counted.

Nucleic acid extraction from drinking water and biofilms. Bulk water DNA and RNA were extracted from the filter sandwiches. For the extraction of DNA and RNA, a modified DNeasy/RNeasy protocol (Qiagen, Hilden, Germany) was used. In this procedure, sandwich filters were cut into pieces and incubated with lysis buffer containing 10 mg/ml lysozyme (Sigma) for 60 min at 37°C (DNA) or 20 min at 20°C (RNA). After a proteinase K digestion (DNA) according to the manufacturer's instructions, the samples were heated to 70°C in a water bath for 20 min (DNA) or 15 min (RNA). After filtration through a polyamide mesh (250-μm mesh size), absolute ethanol was added to the filtrate (filtrate/ethanol ratio, 2:1), and the mixture was applied to the appropriate spin column of the Qiagen kit. Further washing and elution protocols were according to the manufacturer's instructions.

Biofilm swabs were incubated with 220 μl lysis buffer (2× Tris-EDTA) containing 10 mg/ml lysozyme (Sigma) and 15 mg/ml proteinase K (Qiagen) for 20 min at 37°C. AL buffer (350 μl; from the DNeasy kit) or 700 μl RLT buffer (from the RNeasy kit) was added to two replicate swabs, followed by incubation for 5 min at 70°C. The lysate was removed from the swab by a short spindown, and absolute ethanol was added to the lysate (lysate/ethanol ratio, 2:1). The mixture was applied to the appropriate spin column of the kit. After this step, the protocol of the manufacturer was followed. For bulk water or biofilm RNA, a subsequent on-column DNase digestion (RNase-free DNase set; Qiagen, Hilden, Germany) was applied. Nucleic acids were eluted from the columns with DNase/RNase-free water and stored at −20°C. The nucleic acids were quantified using Ribogreen (RNA or single-strand DNA [ssDNA] quantification; Molecular Probes; Invitrogen) or Picogreen (double-strand [dsDNA] quantification; Molecular Probes, Invitrogen) according to Weinbauer et al. (43).

16S rRNA and 16S rRNA gene-based community fingerprints. The PCR amplification of 16S rRNA genes from the extracted nucleic acids was performed using the previously described primers COM1 (5′-CAGCAG CCGCGGTAATAC-3′) and COM2 (5′-CCGTCAATTCCTTTGAGTTT-3′), amplifying positions 519 to 926 of the *Escherichia coli* numbering of the 16S rRNA gene (40). For single-strand separation, a 5′-biotin-labeled forward primer was used according to Eichler et al. (11). From 16S rRNA, reverse transcription was carried out before PCR using the first-strand cDNA synthesis kit (Fermentas, Canada) by following the manufacturer's instructions with the same COM primers. PCR was carried out using 2 ng DNA/cDNA template in a final volume of 50 μl, starting with an initial denaturation for 15 min at 95°C. A total of 30 cycles (30 s at 95°C, 30 s at 55°C, and 1 min at 72°C) was followed by a final elongation for 10 min at 72°C. Amplification was achieved using HotStarTaq DNA polymerase (Qiagen, Hilden, Germany).

For the preparation of ssDNA and community fingerprints, the protocol described by Eichler et al. (11) was slightly modified. Briefly, magnetic streptavidin-coated beads (Promega, Madison, WI) were applied to obtain ssDNA from the PCR amplicons. The quantification of the obtained ssDNA was performed on a 1.5% agarose gel by comparison to a low-molecular-size marker (Invitrogen low-DNA-mass ladder). For SSCP fingerprint analysis, 25 ng of the obtained ssDNA was mixed with gel loading buffer (95% formamide, 10 mM NaOH, 0.25% bromphenol blue, 0.25% xylene cyanol) in a final volume of 7 μl. After incubation for 3 min at 95°C, the ssDNA samples were cooled on ice, loaded onto a nondenaturing polyacrylamide-like gel (0.6× MDE gel solution; Cambrex BioScience, Rockland, ME), and electrophoretically separated at 20°C at 400 V for 18 h on a Macrophor sequencing apparatus (Pharmacia Biotech, Germany). The gel was silver stained according to the method described by Bassam et al. (2). Dried SSCP gels were digitized using an Epson Expression 1600 Pro scanner, and bands with an intensity of >0.1% of the total lane were considered for further statistical analysis. Similarity coefficients were calculated using the Pearson algorithm. Dendrograms were constructed with the neighbor-joining algorithm using GelCompare II software (Applied Maths, Kortrijk, Belgium). Community indices were calculated using the software Primer 6 (Primer-E Ltd., Ivybridge, United Kingdom).

Sequence information from the single bands of the SSCP fingerprints was obtained by following the protocol of Eichler et al. (11).

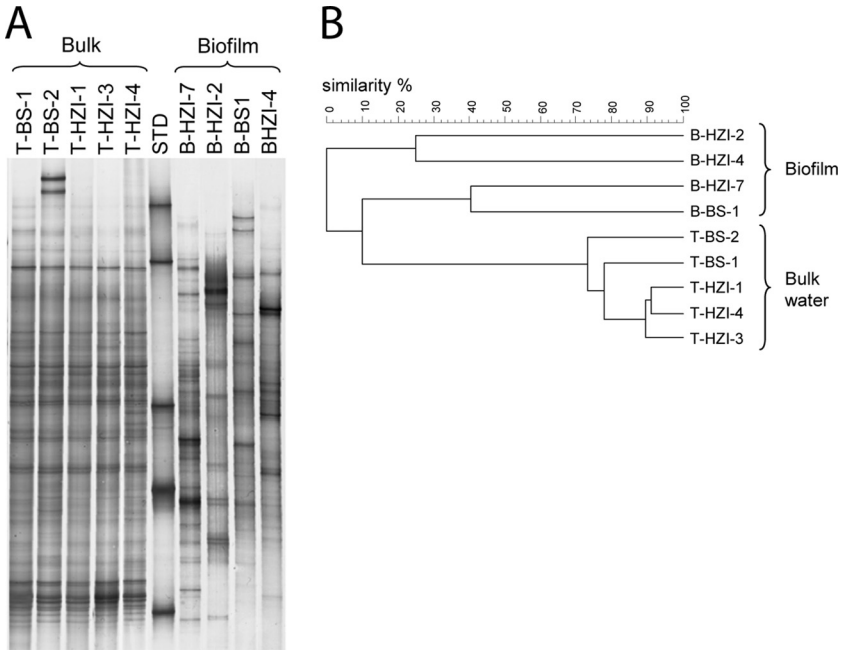

FIG 1 (A) Comparison of 16S rRNA gene-based SSCP fingerprints of bulk water and drinking water biofilm samples. STD, standards. (B) Comparative cluster analysis of 16S rRNA gene-based SSCP fingerprints of bulk water and biofilms.

Briefly, ssDNA bands were excised from the SSCP acrylamide gels and boiled in extraction buffer (10 mM Tris-HCl, 5 mM $MgCl_2$, 5 mM KCl, 0.1% Triton X-100, pH 9). Seven μl of the extraction solution was used in a reamplification PCR with the unbiotinylated COM primers described above. These amplicons were purified (MinElute kit; Qiagen, Hilden, Germany) and subsequently sequenced by cycle sequencing (ABI Prism BigDye Terminator cycle sequencing ready reaction kit; Applied Biosystems, Foster City, CA). Before analysis on an ABI Prism 3100 genetic analyzer, the products were purified using the BigDye Terminator purification kit (Qiagen). The phylogenetic identification of the sequences was done either by the NCBI tool BLAST/blastn (1) for comparison to the closest 16S rRNA gene sequence and for the identification of the closest described relative or the Ribosomal Data Base Project Seqmatch and Classifier tool (8, 42) for the determination of corresponding phyla (RDP release 10, update 18, 25 January 2010). When more than two definite base pair differences existed compared to other phylotypes, we defined a new phylotype.

Nucleotide sequence accession numbers. The partial 16S rRNA gene sequences retrieved from the fingerprints are accessible under the GenBank/EMBL/DDBJ accession numbers FR796543 to FR796698.

RESULTS

General properties of bulk water and biofilm. For all bulk water samples, total bacterial cell counts, CFU on R2A agar, and a set of physical and chemical parameters were determined (see Table S1 in the supplemental material). For the sampling period, no chlorine was detected, and the temperature varied between 12.5 and 23.7°C. Heterotrophic plate counts (HPCs) varied between 0.3 and 556.3 CFU/ml, while direct counts remained rather constant between 1.25×10^5 and 2.57×10^5 cells/ml. The pH was always around 8.4, and the conductivity ranged from 128 to 164 μS/cm, with the exception of the reverse osmosis sample (T-HZI-5), which showed a conductivity of 715 μS/cm. Biofilm samples differed in consistency and color (see Table S2 in the supplemental material). Some samples were slimy and yellow-beige (B-HZI-2), and some were more friable and green (B-HZI-3). Most biofilm samples showed various orange-brown colors with a friable consistency.

Comparison of bacterial community structures in bulk water and biofilm. DNA-based SSCP fingerprints were used to analyze the community structure of biofilm of 8 different sampling sites at the HZI campus and bulk water from the HZI campus and the inner city of Braunschweig (Fig. 1A; also see Fig. S2a in the supplemental material). For all seven bulk water fingerprints, no major differences could be observed, except for two additional intense bands in sample T-BS-2, which was from the inner city of Braunschweig. In contrast, biofilm fingerprints sampled at the 8 different sampling sites were very diverse. Each biofilm fingerprint showed a unique pattern, with sometimes only a few dominating bands. The comparative cluster analysis of bulk water and biofilm fingerprints confirmed the finding that the bulk water fingerprints were very similar to each other, while the biofilm fingerprints were very diverse (Fig. 1b). All bulk water fingerprints clustered closely together; those sampled at the HZI campus had similarities higher than 85%. In contrast, biofilm fingerprints clustered together in two subclusters showing a high diversity with a maximum similarity of 40% to each other.

We calculated rank abundance curves from the DNA-based fingerprints of the bulk water and biofilm samples to compare their overall community structures (Fig. 2). These rank abundance curves were based on the assumption that each band of a fingerprint represents a single phylotype (PT) and the band intensity is proportional to its relative abundance. In the bulk water communities, between 52 (T-BS-2) and 69 (T-HZI-1) phylotypes were found above the detection limit (i.e., relative abundance of 0.1%). The relative abundance of the most abundant phylotype, i.e., rank one, ranged from 6% in sample T-HZI-1 up to 15% in sample T-BS-1. Although biofilm fingerprints differed strongly,

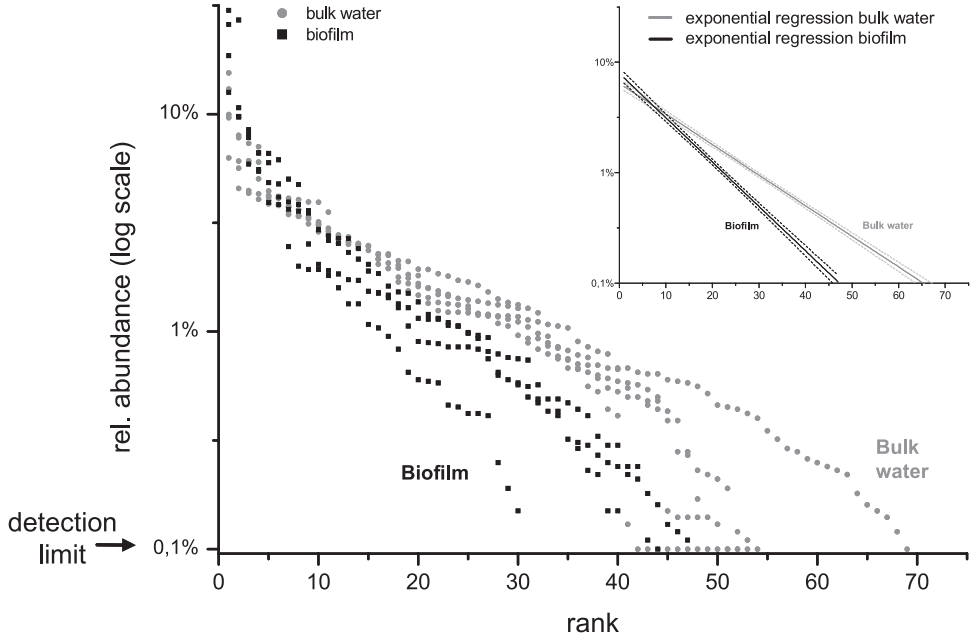

FIG 2 Rank abundance plot of bulk water (gray dots) and biofilm samples (black squares) using relative band intensities from DNA-based fingerprints as a measure for relative abundance. The inset shows the regression analysis of plotted rank abundance curves. Dotted lines indicate 95% confidence bands. For bulk water, $y = 5.8691^{(-0.045015x)}$ and $R^2 = 0.885$; for biofilm, $y = 7.9153^{(-0.092472x)}$ and $R^2 = 0.898$.

their rank abundance curves were quite similar. The biofilm samples had only 30 (B-HZI-2) to 47 phylotypes (B-BS-1) above the detection limit. The most abundant phylotypes reached abundances between 13% (B-BS-1) and 30% (B-HZI-2). The exponential regression analysis of all biofilm and bulk water values and subsequent semilogarithmic plots revealed significantly different slopes and intersections (Fig. 2, inset). The *x* axis intercept, used as an estimator of the richness of communities, indicated a richness of 65.0 for bulk water and 47.3 for biofilms.

Comparison of DNA-based and RNA-based SSCP fingerprints from bulk water and biofilm samples. To compare the present bacterial core communities to the presumably active ones in bulk water, we used DNA-based and RNA-based 16S rRNA (gene) fingerprints, focusing on the five samples collected at the HZI campus which had been in direct contact with the biofilms (see Fig. S2a in the supplemental material). The banding patterns of DNA- and RNA-based fingerprints had low variability; both groups of patterns were substantially different from each other. Accordingly, the comparative cluster analysis of these fingerprints resulted in two clearly separated clusters, one with DNA-based fingerprints and the other with RNA-based fingerprints (see Fig. S2b in the supplemental material).

The comparison of SSCP fingerprints based on the analysis of 16S rRNA and 16S rRNA genes was also done for eight biofilm samples, seven of them from the HZI campus and one (B-BS-1) obtained in the inner city of Braunschweig (Fig. 3A; also see Table S2 in the supplemental material). The high variation of biofilm fingerprints obtained from different sampling sites was observed for DNA- and RNA-based fingerprints. However, similar banding patterns were observed in biofilms sampled at adjacent sampling sites irrespective of the tubing material, i.e., samples from the glass surface (B-HZI-6) and from the steel filter grid of the control window (B-HZI-5). These similar banding patterns were found for both types of fingerprints. In contrast to the bulk water fingerprints, the DNA-based biofilm fingerprints looked more similar to the RNA-based fingerprints of the same sample. Comparative cluster analysis of the biofilm samples showed similarities clearly lower (range, 5 to 60%) than those obtained for bulk water samples, confirming the higher diversity of the biofilm communities (Fig. 3B). DNA- and RNA-based fingerprints of the same sample often clustered together and formed a DNA-RNA subcluster with similarities ranging from 25 to 40%. Additionally, the fingerprints of biofilms collected in the looped fire water mains (B-HZI-3 to B-HZI-6), a circular pipeline, formed a separate subcluster with similarities between 25 and 60%. The subcluster of B-HZI-7 (steel) and B-BS-1 (plastics and PVC), with similarities between 30 and 45%, contained fingerprints of biofilms that both were directly exposed to the municipal water circulation, i.e., not connected to internal circulation (see Table S1 in the supplemental material). Overall, fingerprints of biofilm samples with physically related sampling sites were more similar to each other than fingerprints grown on the same material but on physically unrelated sampling sites, i.e., at least more than 50 m apart and in different buildings.

To understand in detail the differences in the community structure of bulk water and biofilm samples, six different diversity/richness indices were calculated (Table 1) for both types of fingerprints. As we used relative abundance data, all abundances add up to 100% and the diversity indices were calculated using proportions of each species instead of absolute numbers of individuals (13). In general, higher Margalef d and Fisher's α values were obtained for bulk water communities than for biofilm communities on both types of fingerprints. The Pilou evenness J′ and the Simpson 1-λ indices showed similar values for bulk water communities in the DNA-based data and biofilm communities in the RNA-based data, which were always a bit higher than the indices for bulk water communities in the RNA-based data and biofilm

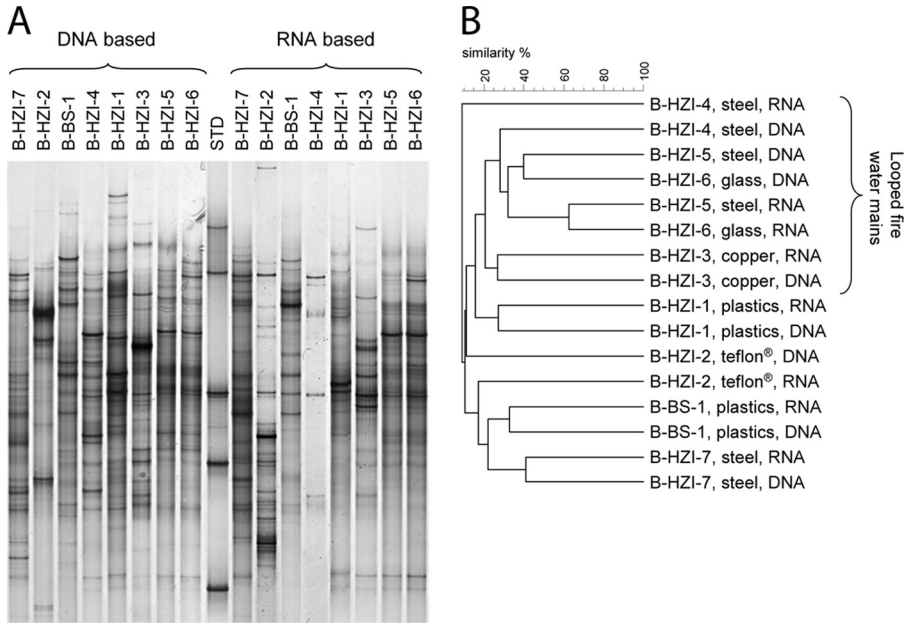

FIG 3 (A) 16S rRNA gene-based SSCP fingerprints of biofilm samples (left side, DNA based) and 16S rRNA-based SSCP fingerprints of biofilm (right side, RNA based). (B) Comparative cluster analysis of DNA- and RNA-based SSCP fingerprints of the biofilm samples.

communities in the DNA-based data. Overall, all biofilm communities showed higher relative abundances of single phylotypes and a reduced richness compared to bulk water communities.

Taxonomic composition of bulk water communities. We obtained a set of 44 unique phylotypes from bulk water fingerprints. Twenty-six phylotypes were obtained from DNA-based fingerprints and 18 phylotypes were from RNA-based fingerprints, with no identical phylotypes among DNA- and RNA-based sequences. The phylogenetic identification of the phylotypes is summarized in Table S3 in the supplemental material. We used a sequence similarity of 90% or higher for the 16S rRNA gene to consider the phylotype to be of aquatic origin. 16S rRNA gene sequence similarities below 90% were regarded as too low to give information on the potential habitat of a PT. Based on these criteria, 75% of the bulk water phylotypes were considered to be of aquatic origin, with most of them being from freshwater habitats. The observed PTs were mainly related to members of taxonomic groups typical for freshwater according to Zwart et al. (45) and Newton et al. (31), such as *Bacteroidetes* (11 PTs; 25%), *Betaproteobacteria* (9 PTs; 20%), *Actinobacteria* (7 PTs; 16%), and *Alphaproteobacteria* (5 PTs; 11%). Small numbers of phylotypes were observed for members of *Cyanobacteria*, *Nitrospira*, *Planctomycetes*, *Gammaproteobacteria*, and the candidate division TM6 (see Table S5 in the supplemental material).

The taxonomic composition of the bacteria from bulk water is given in Fig. 4A using relative abundances estimated from band intensities. For the bulk water, on average 72% (coefficient of variation [CV], ±6.2%) of the bands could be assigned to a specific phylotype. The taxonomic compositions of all bulk water samples were very similar to each other but had no overlap between DNA- and RNA-based fingerprints. DNA-based fingerprints were mainly composed of members of *Bacteroidetes* (12 to 20% sum of relative abundances), *Actinobacteria* (17 to 22%), and *Alphaproteobacteria* (18 to 27%), with the former two phyla being detected almost exclusively in DNA-based fingerprints (Fig. 4A). RNA-based phylotypes belonged mainly to *Betaproteobacteria* (17 to 23%), *Gammaproteobacteria* (10 to 35%), and candidate division TM6 (3 to 16%), whereas the latter two phyla were present only on the RNA-based fingerprints. The two gammaproteobacterial phylotypes found were the most abundant phylotypes in RNA-based fingerprints.

The taxonomic analyses of the bulk water samples of this study

TABLE 1 Mean values of community structure indices for bulk water and biofilm communities calculated from relative abundance data of the SSCP fingerprints

Community	Index CV[a] (%)					
	Richness[b]	Margalef d[c]	Fisher's α[c]	Shannon H′[c]	Pielou eveness J′[c]	Simpson 1-λ[c]
Bulk water (DNA)	64 ± 10	13.72 ± 10	80.73 ± 28	3.45 ± 4	0.83 ± 2	0.97 ± 1
Bulk water (RNA)	60 ± 6	12.86 ± 7	64.97 ± 19	2.98 ± 8	0.73 ± 9	0.91 ± 6
Biofilm (DNA)	54 ± 21	11.40 ± 22	53.33 ± 64	2.94 ± 21	0.74 ± 18	0.89 ± 12
Biofilm (RNA)	54 ± 28	11.45 ± 28	59.30 ± 80	3.23 ± 14	0.81 ± 8	0.94 ± 4

[a] The indices Margalef d and Fisher's α are measures for richness, while the Shannon H′, the Pilou evenness J′, and the Simpson 1-λ are measures for diversity, dominance, and equitability, respectively. Coefficients of variation are given in percentages.
[b] Values were directly retrieved from raw data.
[c] Values were calculated from derived data.

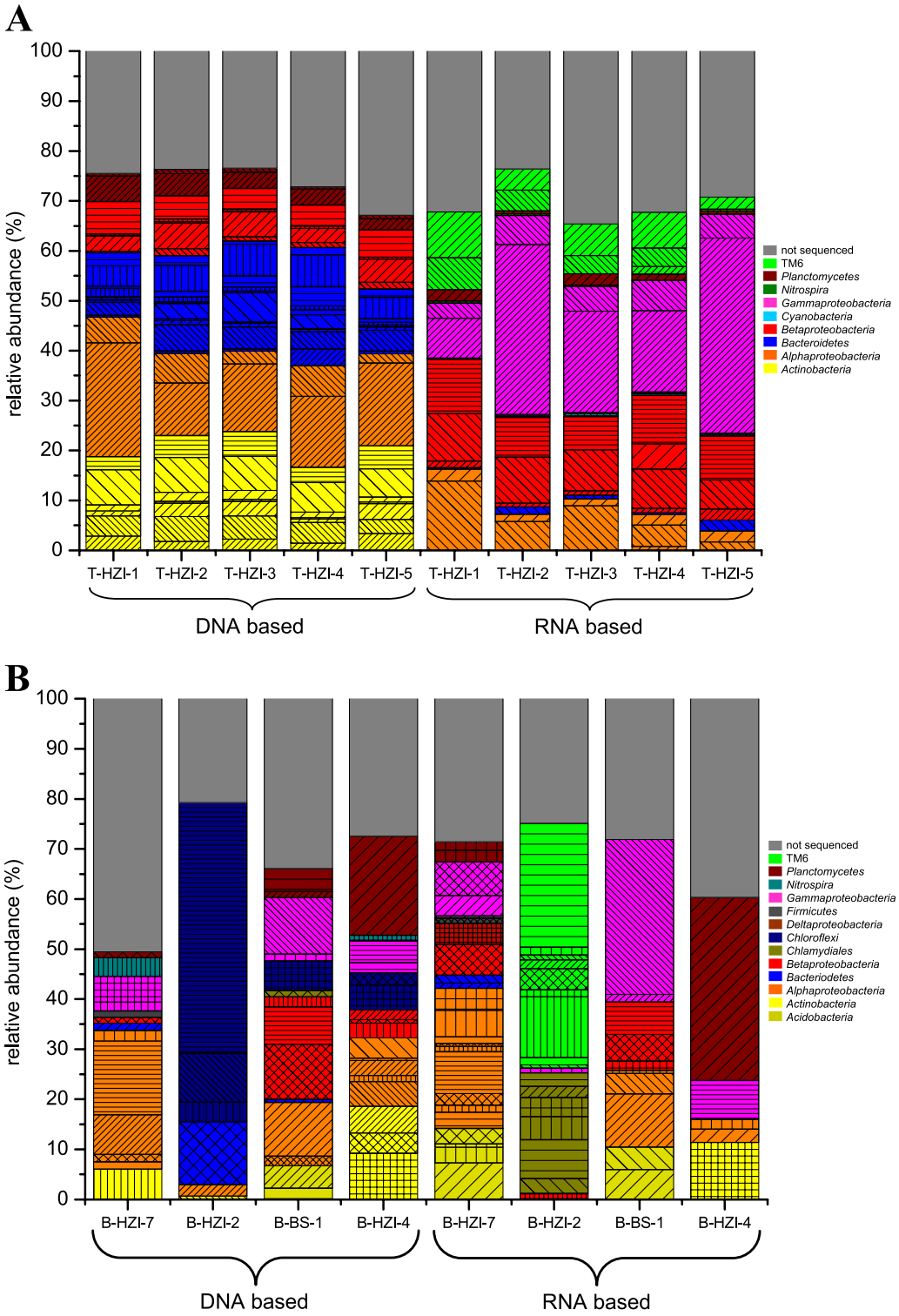

FIG 4 (A) Comparison of relative abundances of the major phylotypes (relative abundances above 1%) found in the bulk water communities. The left part represents the phylotypes from the DNA-based SSCP fingerprints, and the right part represents the phylotypes from the RNA-based SSCP fingerprints. The colors correspond to the major phylogenetic groups of the phylotypes. The differently hatched parts of the stacked bars represent the single phylotypes identified. (B) Comparison of relative abundances of the major phylotypes found in four selected biofilm fingerprints. The biofilms were not directly physically related. The left part represents the phylotypes from the DNA-based SSCP fingerprints, and the right part represents the phylotypes from the RNA-based SSCP fingerprints. The colors correspond to the major phylogenetic groups of the phylotypes. The differently hatched parts of the stacked bars represent the single phylotypes identified.

complement the analyses of two former studies of the same DWDS (11, 21). This allows us to extend the observation period of the bulk water in contact with the mature biofilms by two more sampling periods in 2003 (11) and 2008 (21), thus covering at least partially a period of a total of 6 years, i.e., from 2003 to 2009. For the bulk water, the current study shows a phylum composition similar to that found in the two former studies; concerning phylotype reoccurrence, 34% of the phylotypes of this study could be considered identical to those of former studies when a distinction of 0 to 3 nucleotides (nt) (corresponding to a 16S rRNA similarity of 99% or higher) is applied, and we found a reoccurrence of 41% based on a 4- to 6-nt distinction (98% similarity) (see Table S3 in the supplemental material).

Taxonomic composition of biofilm communities. A set of 112 unique phylotypes was obtained from both types of fingerprints from four physically unrelated biofilm samples (see Table S4 in the supplemental material). Fifty-five phylotypes occurred only in DNA-based fingerprints, and 44 phylotypes occurred only in RNA-based fingerprints, whereas 13 phylotypes were found in both types of fingerprints (Fig. 4B; also see Table S5 in the supplemental material). Sequence comparison to all bulk water phylotypes revealed no congruence between phylotypes from bulk water and biofilm communities (see Fig. S3 in the supplemental material). Compared to the former studies of this DWDS (11, 21), only a phylotype related to *Nitrospira moscoviensis* was redetected at a low abundance by DNA analyses of biofilm samples (PT B018; 100% 16S rRNA similarity to a PT retrieved from RNA of bulk water in 2003) (Fig. 4B; also see Table S4 in the supplemental material). Using the same criteria as that for the bulk water samples, 17% of all biofilm phylotypes were considered to be of aquatic origin, 9% were considered to be of biofilm origin, and 32% were considered to be of soil, sludge, or sediment origin. In the case of aquatic origin, many of the phylotypes had highest similarities to phylotypes found in either wastewater or water treatment plants. Most of the biofilm phylotypes (Fig. 4B) belonged to the *Alphaproteobacteria* (28 PTs; 26%), followed by *Gammaproteobacteria* (12 PTs; 11%) and the candidate division TM6 (12 PTs; 11%). Additionally, we found *Chlamydiales* (10 PTs; 9%) and *Betaproteobacteria* (10 PTs; 9%). Taxonomic groups with fewer than 10 phylotypes were *Acidobacteria*, *Planctomycetes*, *Firmicutes*, *Actinobacteria*, *Chloroflexi*, *Bacteroidetes*, and *Nitrospira* (see Table S5 in the supplemental material). Phylotypes belonging to *Chlamydiales* and the candidate division TM6 were found mainly in sample B-HZI-2, which was sampled from a Teflon tube attached to the tap. Furthermore, this biofilm was the only one showing pronounced differences between the taxonomic composition of DNA- and RNA-based fingerprints. In this biofilm community, based on DNA fingerprints, only three phylotypes belonging to the phylum *Chloroflexi* represented approximately two thirds of phylotypes, while in other biofilms the *Chloroflexi* phylotypes accounted for a maximum abundance of only 7.4%. In the RNA-based fingerprints of this biofilm sample, a completely different set of phylotypes was observed. Overall, each biofilm fingerprint represented an individual bacterial community with a unique taxonomic composition that had some similarities between DNA- and RNA-based fingerprints.

DISCUSSION

Comparison of bacterial community structures of bulk water and biofilms. The physical and chemical bulk water parameters recorded during our study were comparable to those reported regularly by the local drinking water supplier Harzwasserwerke; the analyzed samples therefore are considered to be representative of Braunschweig's drinking water. The high similarity of all bulk water fingerprints demonstrated the stability of the overall community structure of the drinking water bacteria with little spatial variation (see Fig. S2b in the supplemental material). The drinking water core community in this DWDS was independent from the sampling site, as confirmed by DNA- and RNA-based fingerprints. These findings were consistent with Eichler et al. (11), who sampled the same drinking water supply system along the production line from the reservoirs to the tap. Overall, we conclude that the bacterial core community was not affected by minor changes in the physicochemical conditions of the bulk water, indicating a high resilience of this community across the distribution network.

In contrast to those for bulk water, biofilm fingerprints showed large differences, indicating a high spatial variability of the bacterial core communities of the biofilms (Fig. 3A). Each biofilm showed a unique fingerprint pattern, indicating that each biofilm consisted of a unique community. Based on the cluster analyses of the fingerprints, relationships between biofilm core communities were more pronounced in correspondence to the vicinity of biofilms than to the support material. For example, all fingerprints of biofilms that were sampled in the looped fire water mains (B-HZI-3 to B-HZI-6) had their own subcluster, even though these biofilms were grown on different surface materials (copper, steel, and glass). This effect was especially apparent in the control window subcluster (B-HZI-5 and B-HZI-6). Here, the RNA-based fingerprints of biofilms grown on steel or glass clustered more closely together than their corresponding DNA-based fingerprints. Also, the fingerprints of biofilms grown in the municipal water (B-BS-1 and B-HZI-7) showed similarities despite different surface materials (steel and PVC). The observed similarity of physically related biofilms and the low dependency of the community structure on the surface material could be explained by the mutual influence of adjacent biofilm communities. Although the first colonization of surfaces has been shown to be dependent on the surface material (10, 24), an adjacent, years-long coexistence may lead to the mutual influence of biofilms by the exchange of bacteria. If the surface is covered first by a surface-specific biofilm, it is conceivable that it is later overgrown by a nearby biofilm community that is more independent from the surface material. From our observations, we hypothesize that during several years physically related biofilm communities will show similar community structures. Our observations are corroborated by Martiny et al. (29), who show in their model DWDS that after 3 years most biofilms from different sampling positions clustered together, indicating a homogeneous community structure.

The mean slope of rank abundance curves for DNA-based bulk water and biofilm fingerprints differed substantially, demonstrating considerable structural differences between the communities (Fig. 2). For the bulk water, our rank abundance data suggest that there is a wide variety of low-abundance phylotypes, which were at or below our detection limit of 0.1% relative abundance. This is consistent with other studies of pelagic bacterial communities, including drinking water (6, 11, 34, 36). In contrast to the bulk water community, each biofilm community used for these calculations might consist, as demonstrated, of a unique set of bacterial species. Nevertheless, all biofilm rank abundance curves showed the same trend for slope and axis interception. This behavior sug-

gests, with respect to the diversity and structure of biofilm communities, that there are similar mechanisms structuring these communities in DWDS, i.e., all biofilms provide a similar number of niches but are filled with different species. The same overall structure for drinking water biofilms was also observed in a recent study using pyrosequencing (19), i.e., a rapid decrease of abundant species with a long "tail" of rare species.

In general, DNA- and RNA-based fingerprints of biofilms were much more similar to each other than were bulk water fingerprints. The RNA-DNA relatedness within the biofilm fingerprints indicate that in biofilms bacteria are growing that are also highly active, finally leading to higher abundances in the DNA-based fingerprints. We assume that only those bacteria that can actively contribute to the succession of the biofilm were successful in colonizing biofilms, while bacteria that cannot fill perfectly the narrow niches in biofilms vanished over time. This process would lead to a lower richness in biofilm than in the corresponding bulk water and explains why we observed lower richness values for biofilms than for bulk water (Table 1).

Besides different levels of activity, other factors could have led to a distinct RNA-DNA similarity in water and biofilm, e.g., oxidative stress. For low-nutrient environments, it was shown that bacteria reduce their RNA content in the stationary phase or under starvation in the presence of oxidative stress, whereas the RNA content remained high under starvation in anoxic or low-oxygen environments with low oxidative stress (5). In the studied drinking water, oxidative stress is high due to high oxygen concentrations and the presence of chlorine residues. Since we can assume that the oxidative stress is far higher in the bulk water than in the biofilm, the discrepancy between the phylotypes derived from RNA and DNA could also be attributed, at least to a certain extent, to oxidative stress contributing to RNA degradation for bacteria in the bulk water. On the other hand, reduced oxidative stress and improved nutrient conditions could have allowed a high RNA level for bacteria in biofilm. For the latter, in addition to reduced oxidative stress, growth due to better nutrient conditions could have contributed to an increased RNA content for the biofilm bacteria; in this case, activity and oxidative stress could be assumed to have a combined effect.

Comparison of taxonomic compositions of bulk water and biofilm communities. In contrast to bulk water, the majority of biofilm phylotypes were considered to be of soil, sludge, sediment, or biofilm origin. Members of the key genera *Rhizobiales*, *Nitrospira*, and *Thiobacillus*, which we found in drinking water biofilms, are known to contribute to the biogeochemical cycling of nitrogen or sulfur. Many other uncultured bacteria with high similarities to denitrifying species also were found in these biofilms. This suggests that the species in biofilms form a system of complex interactions to build a community metabolism. Although each biofilm consists of a set of unique phylotypes, these phylotypes belonged to classes which were present in most biofilms in comparable abundances, especially members of the *Alphaproteobacteria*, *Gammaproteobacteria*, and *Deltaproteobacteria* (Fig. 4B; also see Fig. S3 in the supplemental material). This indicates that different biofilm communities provide niches with similar conditions which are filled by different species belonging to the same class (see Fig. S4a and b and Table S5).

Seven different uncultured phylotypes of the *Chlamydiales* with high 16S rRNA sequence similarity to members of the *Parachlamydiaceae*, such as *Parachlamydia acanthamoebae*, *Protochlamydia naegleriophila*, and *Neochlamydia hartmannellae* (biofilm samples B-HZI-2 and B-BS-1), could be of relevance as potential pathogens. *Parachlamydiaceae* have been reported from patients with community-acquired pneumonia (28) and are known to enter and replicate within human macrophages (15, 16).

Bulk water and biofilm community structures were characterized by large differences observed with both types of fingerprints. The phylotype B018, closely related to *Nitrospira moscoviense*, was the only phylotype that was observed in the biofilm and in bulk water, the latter having been observed in the study of Eichler et al. (11). Martiny et al. (29) observed *N. moscoviense* as a major fraction in biofilm and bulk water. In our studies, *N. moscoviense* was found at low abundance in biofilm of this study and in bulk water in 2003 (11), but it was not detected in the bulk water of the present study. Thus, it can be concluded that no major establishment of members of the core community of the bulk water occurred in the biofilm or vice versa. The current model of abundant and rare members describes the bacterioplankton community in pelagic ecosystems, consisting of a core community with few taxa that are highly abundant and a seed bank with nearly infinite numbers of low-abundance phylotypes (18, 20, 33). As a biofilm provides niches that differ from those in the bulk water, we hypothesize that the low-abundance bacteria from the bulk water function as a seed bank for the biofilm. This hypothesis represents a mechanism for the formation of drinking water biofilms which could be tested using high-resolution community analyses by next-generation sequencing (14, 30).

ACKNOWLEDGMENTS

We thank Julia Strömpl and Josefin Draheim for their excellent technical support.

This work was supported by funds from the European Commission for the HEALTHY WATER project (FOOD-CT-2006-036306).

We are solely responsible for the content of this publication. It does not represent the opinion of the European Commission. The European Commission is not responsible for any use that might be made of data appearing herein.

REFERENCES

1. **Altschul SF, Gish W, Miller W, Myers EW, Lipman DJ.** 1990. Basic local alignment search tool. J. Mol. Biol. **215**:403–410.
2. **Bassam BJ, Caetano-Anollés G, Gresshoff PM.** 1991. Fast and sensitive silver staining of DNA in polyacrylamide gels. Anal. Biochem. **196**:80–83.
3. **Batté M, et al.** 2003. Biofilms in drinking water distribution systems. Rev. Environ. Sci. Biotechnol. **2**:147–168.
4. **Berry D, Xi C, Raskin L.** 2006. Microbial ecology of drinking water distribution systems. Curr. Opin. Biotechnol. **17**:297–302.
5. **Brettar I, Christen R, Höfle MG.** 2012. Analysis of bacterial core communities in the central Baltic by comparative RNA-DNA-based fingerprinting provides links to structure-function relationships. ISME J. **6**:195–212.
6. **Brettar I, Höfle MG.** 2008. Molecular assessment of bacterial pathogens–a contribution to drinking water safety. Curr. Opin. Biotechnol. **19**:274–280.
7. **Buswell CM, et al.** 1998. Extended survival and persistence of *Campylobacter* spp. in water and aquatic biofilms and their detection by immunofluorescent-antibody and -rRNA staining. Appl. Environ. Microbiol. **64**: 733–741.
8. **Cole JR, et al.** 2009. The Ribosomal Database Project: improved alignments and new tools for rRNA analysis. Nucleic Acids Res. **37**:D141–D145.
9. **Colwell RR, Grimes DJ.** 2000. Nonculturable microorganisms in the environment. ASM Press, Washington DC.
10. **Donlan RM.** 2002. Biofilms: microbial life on surfaces. Emerg. Infect. Dis. **8**:881–890.

11. **Eichler S, et al.** 2006. Composition and dynamics of bacterial communities of a drinking water supply system as assessed by RNA- and DNA-based 16S rRNA gene fingerprinting. Appl. Environ. Microbiol. **72**:1858–1872.
12. **Feazel LM, et al.** 2009. Opportunistic pathogens enriched in showerhead biofilms. Proc. Natl. Acad. Sci. USA **106**:16393–16399.
13. **Fisher RA, Corbet AS, Williams CB.** 1943. The relation between the number of species and the number of individuals in a random sample of an animal population. Animal Ecol. **12**:42–58.
14. **Fuhrman JA.** 2009. Microbial community structure and its functional implications. Nature **459**:193–199.
15. **Greub G.** 2009. *Parachlamydia acanthamoebae*, an emerging agent of pneumonia. Clin. Microbiol. Infect. **15**:18–28.
16. **Greub G, Mege J-L, Raoult D.** 2003. *Parachlamydia acanthamoebae* enters and multiplies within human macrophages and induces their apoptosis. Infect. Immun. **71**:5979–5985.
17. **Henne K, Kahlisch L, Draheim J, Brettar I, Höfle MG.** 2008. Polyvalent fingerprint based molecular surveillance methods for drinking water supply systems. Water Sci. Technol. Water Supply **8**:527.
18. **Höfle M, Kirchman D, Christen R, Brettar I.** 2008. Molecular diversity of bacterioplankton: link to a predictive biogeochemistry of pelagic ecosystems. Aquat. Microb. Ecol. **53**:39–58.
19. **Hong P-Y, et al.** 2010. Pyrosequencing analysis of bacterial biofilm communities in water meters of a drinking water distribution system. Appl. Environ. Microbiol. **76**:5631–5635.
20. **Huber JA, et al.** 2007. Microbial population structures in the deep marine biosphere. Science **318**:97–100.
21. **Kahlisch L, Henne K, Groebe L, Brettar I, Höfle MG.** 2012. Assessing the viability of bacterial species in drinking water by combined cellular and molecular analyses. Microb. Ecol. **63**:383–397.
22. **Keinänen-Toivola MM, Revetta RP, Domingo JWS.** 2006. Identification of active bacterial communities in a model drinking water biofilm system using 16S rRNA-based clone libraries. FEMS Microbiol. Lett. **257**:182–188.
23. **Kerkhof L, Kemp P.** 1999. Small ribosomal RNA content in marine Proteobacteria during non-steady-state growth. FEMS Microbiol. Ecol. **30**:253–260.
24. **Kerr CJ, Osborn KS, Rickard AH, Robson GD, Handley PS.** 2003. Biofilms in water distribution systems, p 757–776. *In* Mara D, Horan N (ed), Water and wastewater engineering. Academic Press, London, United Kingdom.
25. **LeChevallier MW, Babcock TM, Lee RG.** 1987. Examination and characterization of distribution system biofilms. Appl. Environ. Microbiol. **53**:2714–2724.
26. **Lehtola MJ, et al.** 2004. Microbiology, chemistry and biofilm development in a pilot drinking water distribution system with copper and plastic pipes. Water Res. **38**:3769–3779.
27. **Mahmood S, Paton GI, Prosser JI.** 2005. Cultivation-independent in situ molecular analysis of bacteria involved in degradation of pentachlorophenol in soil. Environ. Microbiol. **7**:1349–1360.
28. **Marrie TJ, Raoult D, La Scola B, Birtles RJ, de Carolis E.** 2001. Legionella-like and other amoebal pathogens as agents of community-acquired pneumonia. Emerg. Infect. Dis. **7**:1026–1029.
29. **Martiny AC, Jørgensen TM, Albrechtsen H-J, Arvin E, Molin S.** 2003. Long-term succession of structure and diversity of a biofilm formed in a model drinking water distribution system. Appl. Environ. Microbiol. **69**:6899–6907.
30. **Metzker ML.** 2010. Sequencing technologies–the next generation. Nat. Rev. Genet. **11**:31–46.
31. **Newton RJ, Jones SE, Eiler A, McMahon KD, Bertilsson S.** 2011. A guide to the natural history of freshwater lake bacteria. Microbiol. Mol. Biol. Rev. **75**:14–49.
32. **Parsek MR, Singh PK.** 2003. Bacterial biofilms: an emerging link to disease pathogenesis. Annu. Rev. Microbiol. **57**:677–701.
33. **Pedrós-Alió C.** 2006. Marine microbial diversity: can it be determined? Trends Microbiol. **14**:257–263.
34. **Poitelon J-B, et al.** 2009. Assessment of phylogenetic diversity of bacterial microflora in drinking water using serial analysis of ribosomal sequence tags. Water Res. **43**:4197–4206.
35. **Prosser JI, Jansson J, Liu W-T.** 2010. Nucleic-acid-based characterization of community structure and function, p 63–86. *In* Liu WT, Janson JK (ed), Environmental molecular microbiology. Caister Academic Press, Norfolk, United Kingdom.
36. **Revetta RP, Pemberton A, Lamendella R, Iker B, Santo Domingo JW.** 2010. Identification of bacterial populations in drinking water using 16S rRNA-based sequence analyses. Water Res. **44**:1353–1360.
37. **Rittman BE.** 1982. The effect of shear stress on biofilm loss rate. Biotechnol. Bioeng. **24**:501–506.
38. **Rogers J, Dowsett AB, Dennis PJ, Lee JV, Keevil CW.** 1994. Influence of temperature and plumbing material selection on biofilm formation and growth of *Legionella pneumophila* in a model potable water system containing complex microbial flora. Appl. Environ. Microbiol. **60**:1585–1592.
39. **Schwartz T, Hoffmann S, Obst U.** 1998. Formation and bacterial composition of young, natural biofilms obtained from public bank-filtered drinking water systems. Water Res. **32**:2787–2797.
40. **Schwieger F, Tebbe CC.** 1998. A new approach to utilize PCR-single-strand-conformation polymorphism for 16S rRNA gene-based microbial community analysis. Appl. Environ. Microbiol. **64**:4870–4876.
41. **Stoodley P, Sauer K, Davies DG, Costerton JW.** 2002. Biofilms as complex differentiated communities. Annu. Rev. Microbiol. **56**:187–209.
42. **Wang Q, Garrity GM, Tiedje JM, Cole JR.** 2007. Naive Bayesian classifier for rapid assignment of rRNA sequences into the new bacterial taxonomy. Appl. Environ. Microbiol. **73**:5261–5267.
43. **Weinbauer MG, Fritz I, Wenderoth DF, Höfle MG.** 2002. Simultaneous extraction from bacterioplankton of total RNA and DNA suitable for quantitative structure and function analyses. Appl. Environ. Microbiol. **68**:1082–1087.
44. **Williams MM, Braun-Howland EB.** 2003. Growth of *Escherichia coli* in model distribution system biofilms exposed to hypochlorous acid or monochloramine. Appl. Environ. Microbiol. **69**:5463–5471.
45. **Zwart G, Crump BC, Kamst-van Agterveld MP, Hagen F, Han SK.** 2002. Typical freshwater bacteria: an analysis of available 16S rRNA gene sequences from plankton of lakes and rivers. Aquat. Microb. Ecol. **28**:141–155.